



# Finite element Hartree–Fock calculations in three dimensions for atoms and small molecules



Moritz Braun\*

Department of Physics, University of South Africa, P O Box 392, 0003, UNISA, South Africa

## ARTICLE INFO

### Article history:

Received 2 October 2013

Received in revised form 15 January 2014

### Keywords:

Method of finite elements

Python

Hartree–Fock

## ABSTRACT

The present contribution describes a three dimensional finite element approach to the solution of the closed shell Hartree–Fock equations for small molecules. The computational method used to perform such three dimensional finite element Hartree–Fock calculations is based on the use of a factorized Green's function for both the solution of the three dimensional Schrödinger-type equations as well as of the Poisson equation. Results of such calculations are reported for the helium atom, the beryllium atom, and the three molecules methane, water and ammonia and are compared with highly accurate literature values for the atoms and the results of Gaussian basis set calculations performed with NWChem for the molecules.

© 2014 Elsevier B.V. All rights reserved.

## 1. Introduction

Efficient and reliable methods to solve the three-dimensional Schrödinger equation are important as input for density functional and Hartree–Fock calculations. To judge the accuracy of calculations using Gaussian basis functions a comparison with methods having less basis set dependency is desirable. The finite element method [1] could be a candidate for such a method, since its convergence can be improved systematically and the grid can be adjusted based on the requirements of the problem.

Another disadvantage of using Gaussian basis functions is, that the behavior of the orbitals in the asymptotic region is incorrect. This long range behavior is for example important for modeling the charge densities in the vicinity to surfaces that are investigated by scanning tunnel microscopy or similar techniques. This problem does not occur when using the method of finite elements.

Two-dimensional finite element Hartree–Fock calculations have been done already some time ago [2,3]. Three-dimensional finite element Hartree–Fock calculations are more difficult due to the increased number of basis functions and the Coulomb potential being more singular in three dimensions and they have only recently been undertaken [4], and were limited to using first order finite elements.

In this paper results of three dimensional finite element calculations using interpolation polynomials of order  $p = 3$  and  $p = 4$  for a number of atoms and molecules will be presented. Special numerical methods developed to render such calculations feasible are discussed in some detail.

The remainder of the paper is organized as follows. In Section 2 the closed shell Hartree–Fock equations are sketched, the application of the method of finite elements is laid out and it is explained in some detail, how the matrix elements of the Hartree and exchange potentials are evaluated in the finite element basis. In Section 3 some details of the computation,

\* Tel.: +27 124298006; fax: +27 124293643.

E-mail address: [moritz.braun@gmail.com](mailto:moritz.braun@gmail.com).

such as the choice of the finite element grid and the programming language and libraries used are given. Finally in Section 4 results obtained for the atoms helium and beryllium as well as for the molecules methane, water and ammonia are given.

## 2. Method

### 2.1. The closed shell Hartree–Fock method

In the following energies will be measured in units of 1 Hartree = 27.2 eV and distances in  $a_{\text{Bohr}} = 5.29 \times 10^{-11}$  m. Thus the quantum mechanical Hamiltonian for a molecule consisting of  $N$  electrons at positions  $\mathbf{r}_i$ ,  $i = 1, \dots, N$  and  $M$  stationary nuclei at positions  $\mathbf{R}_j$ ,  $j = 1, \dots, M$  is in the Born–Oppenheimer approximation given by

$$H = -\sum_{i=1}^N \frac{1}{2} \nabla_i^2 + \sum_{i>j=1}^N \frac{1}{|\mathbf{r}_i - \mathbf{r}_j|} - \sum_{i=1}^N \sum_{j=1}^M \frac{Z_j}{|\mathbf{r}_i - \mathbf{R}_j|} + \sum_{i>j=1}^M \frac{Z_i Z_j}{|\mathbf{R}_i - \mathbf{R}_j|}. \quad (1)$$

In the following we drop the constant Coulomb repulsion between the nuclei.

The closed shell Hartree–Fock (CSHF) method [5] is based on a variational calculation for the trial wave function

$$\Phi = \mathcal{A} \left| \psi_1(\mathbf{r}_1) \left| \frac{1}{2} \right\rangle_1 \psi_1(\mathbf{r}_2) \left| -\frac{1}{2} \right\rangle_2 \psi_2(\mathbf{r}_3) \left| \frac{1}{2} \right\rangle_3 \psi_2(\mathbf{r}_4) \left| -\frac{1}{2} \right\rangle_4 \cdots \psi_{N/2}(\mathbf{r}_{N-1}) \left| \frac{1}{2} \right\rangle_{N-1} \psi_{N/2}(\mathbf{r}_N) \left| -\frac{1}{2} \right\rangle_N \right\rangle, \quad (2)$$

where  $\mathcal{A}$  is the antisymmetrization operator that converts a product of wave functions into a Slater determinant, the pairwise identical single particle wave functions assigned to the  $j$ th electron are denoted by  $\psi_i(\mathbf{r}_j)$  and  $|\pm \frac{1}{2}\rangle_j$  refer to spin-up/spin-down spinors. It is evident that all pairs of spins are in singlet states. Therefore the CSHF method only works for even  $N$ .

The Hartree–Fock equations for  $N/2$  single particle wave functions  $\psi_i$  are obtained from  $H_{\text{HF}}\psi_i = e_i\psi_i$  with

$$H_{\text{HF}}\psi_i = -\frac{1}{2} \nabla^2 \psi_i(\mathbf{r}) - \sum_{j=1}^M \frac{Z_j}{|\mathbf{r} - \mathbf{R}_j|} \psi_i(\mathbf{r}) + \int d^3r' \frac{2 \sum_{l=1}^{N/2} |\psi_l(\mathbf{r}')|^2}{|\mathbf{r} - \mathbf{r}'|} \psi_i(\mathbf{r}) - \int d^3r' \frac{\sum_{l=1}^{N/2} \psi_l(\mathbf{r}) \psi_l^*(\mathbf{r}')}{|\mathbf{r} - \mathbf{r}'|} \psi_i(\mathbf{r}') \quad (3)$$

or, more succinctly,

$$H_{\text{HF}}\psi_i = \{T + V_N + V_H + V_X\} \psi_i, \quad (4)$$

where the four operators correspond to the four terms in Eq. (3). Since we are only considering bound states in the absence of a magnetic field, the eigenfunctions can be chosen as real-valued and the complex conjugation is dropped for the remainder of the paper.

### 2.2. Application of the method of finite elements to the Hartree–Fock equation

Expanding a solution of the Hartree–Fock equation in terms of the finite element basis, i.e.

$$\psi(\mathbf{r}) = \sum_{j=1}^N v_j F_j(\mathbf{r}),$$

we obtain the generalized eigenvalue problem

$$(\mathbf{T} + \mathbf{V}_N + \mathbf{V}_H + \mathbf{V}_X) \mathbf{v} = E \mathbf{U} \mathbf{v}, \quad (5)$$

where the bold face capital letters refer to finite element matrices. The matrices  $\mathbf{T}$ ,  $\mathbf{V}_N$ ,  $\mathbf{V}_H$  and  $\mathbf{U}$  are sparse, while  $\mathbf{V}_X$  is not sparse due to the non-local nature of the exchange potential.

The above generalized eigenvalue problem could be solved as is, but due to having very large eigenvalues the method of choice for such problems, the Jacobi–Davidson method [6,7] will converge rather slowly.

The above eigenvalue problem can be rewritten as

$$(\mathbf{V}_N + \mathbf{V}_H + \mathbf{V}_X) \mathbf{v} = (E \mathbf{U} - \mathbf{T}) \mathbf{v}, \quad (6)$$

which leads to

$$(E \mathbf{U} - \mathbf{T})^{-1} (\mathbf{V}_N + \mathbf{V}_H + \mathbf{V}_X) \mathbf{v} = \lambda \mathbf{v}, \quad (7)$$

and allows the determination of one eigenstate at a time by finding  $E$  such that the largest, second largest eigenvalue and so on is unity. This is however not efficient, if more than just a few eigenvalues are desired.

A more efficient formulation is obtained by subtracting  $E_0 \mathbf{U} \mathbf{v}$  from both sides of Eq. (5) and multiplying it by  $-(E_0 \mathbf{U} - \mathbf{T})^{-1}$  to yield

$$[\mathbb{1} - (E_0 \mathbf{U} - \mathbf{T})^{-1} (\mathbf{V}_N + \mathbf{V}_H + \mathbf{V}_X)] \mathbf{v} = -(E - E_0)(E_0 \mathbf{U} - \mathbf{T})^{-1} \mathbf{U} \mathbf{v}. \quad (8)$$

If we choose  $E_0$  to be smaller than the lowest eigenvalue of the Hartree–Fock equation, it can be shown, that the eigenvalues of the operator on the LHS of Eq. (8) are all between 0 and 1 and thus the Jacobi–Davidson method converges more rapidly for the bound states we are interested in.

From the above it is clear, that the speed of a method based on the transformation discussed above will crucially depend on a computationally efficient way to represent Green's function  $(E_0 \mathbf{U} - \mathbf{T})^{-1}$ . For three dimensional finite element calculations, the matrices are of order  $\mathcal{N} \approx 10^4 - 10^6$  and LU factorization is virtually impossible. However, factorization of the finite element matrices  $\mathbf{U}$  and  $\mathbf{T}$  using their tensor product structure, which in turn depends on using a tensor mesh that is aligned with the axes, leads to a very efficient representation of Green's function [8–10] as described in the following.

Due to the product form of the interpolation polynomials, the finite element matrices  $\mathbf{U}$  and  $\mathbf{T}$  can be written as

$$\mathbf{U} = u_x \otimes u_y \otimes u_z, \quad (9)$$

$$\mathbf{T} = t_x \otimes u_y \otimes u_z + u_x \otimes t_y \otimes u_z + u_x \otimes u_y \otimes t_z. \quad (10)$$

Here the matrices with indices  $x$ ,  $y$  and  $z$  are one dimensional finite element matrices and the tensor product indicated by  $\otimes$  is to be understood as the tensor product between the matrices considered as linear maps. The same notation has been used in the references given in the previous paragraph.

Factoring out  $\mathbf{U}$  yields

$$E_0 \mathbf{U} - \mathbf{T} = \mathbf{U}(E_0 \mathbb{1} - \mathbf{U}^{-1} \mathbf{T}) = \mathbf{U} \left( E_0 \mathbb{1} - \left\{ u_x^{-1} k_x \otimes \mathbf{1}_y \otimes \mathbf{1}_z + \mathbf{1}_x \otimes u_y^{-1} k_y \otimes \mathbf{1}_z + \mathbf{1}_x \otimes \mathbf{1}_y \otimes u_z^{-1} k_z \right\} \right). \quad (11)$$

The eigenvectors of the matrix in round brackets can be expressed as tensor products of those for  $h_x = u_x^{-1} k_x$ ,  $h_y = u_y^{-1} k_y$  and  $h_z = u_z^{-1} k_z$ , resulting in

$$(E_0 \mathbb{1} - \mathbf{U}^{-1} \mathbf{T}) \mathbf{u}_i \otimes \mathbf{v}_j \otimes \mathbf{w}_k = (E_0 - \lambda_i - \mu_j - \nu_k) \mathbf{u}_i \otimes \mathbf{v}_j \otimes \mathbf{w}_k. \quad (12)$$

Since the eigenpairs of the above operator are known, its inverse allows for an *explicit* and *efficient* construction, and the eigenpairs of the kinetic energy operator are adopted to the singularities of the problem encoded in the finite element grid.

### 2.3. Treatment of Hartree and exchange potentials

Because of the procedure for determining the eigenpairs described above, only multiplication by the finite element matrices corresponding to the various potentials is required. In the following

$$\mathbf{v}^{(i)}, \quad i = 1 \dots N/2$$

denote the finite element vectors corresponding to the wave functions  $\psi_i(\mathbf{r})$ .

For the Hartree potential we avoid the integration over the density appearing in the definition

$$V_H(\mathbf{r}) = \int d^3 r' \frac{2 \sum_{i=1}^{N/2} \psi_i(\mathbf{r}')^2}{|\mathbf{r} - \mathbf{r}'|} \quad (13)$$

by instead solving the Poisson equation

$$-\nabla^2 V_H = 4\pi \rho \quad (14)$$

with

$$\rho(\mathbf{r}) = 2 \sum_{i=1}^{N/2} \psi_i(\mathbf{r})^2. \quad (15)$$

Using the method of finite elements and the Galerkin approach this requires the solution of the linear equation

$$\mathbf{L} \mathbf{v}_H = 4\pi \mathbf{w} \quad (16)$$

with  $\mathbf{L} = 2\mathbf{T}$ ,

$$w_j = \int F_j(\mathbf{r}) \rho(\mathbf{r}) d^3 r, \quad (17)$$

and where  $\mathbf{v}_H$  is the finite element vector corresponding to the Hartree potential. This can be solved using Green's function discussed above with  $E = 0$  and also efficiently using the factorization approach. However for our calculations we replace

the exact charge density  $\rho$  above by its interpolant, which is defined by the values  $\mathbf{n}$  at the nodes of the finite element grid. This is easier to evaluate resulting in

$$\mathbf{L}\mathbf{v}_H = 4\pi\mathbf{U}\mathbf{n} \quad (18)$$

with

$$n_j = 2 \sum_{i=1}^{N/2} |v_j^{(i)}|^2. \quad (19)$$

The exchange term is more complex, but again replacing the integrals by the solutions of Poisson equations with suitable right hand sides one obtains

$$V_X\psi(\mathbf{r}) = - \sum_{i=1}^{N/2} W_i(\mathbf{r})\psi_i(\mathbf{r}) \quad (20)$$

with

$$-\nabla^2 W_i(\mathbf{r}) = 4\pi\psi_i(\mathbf{r})\psi(\mathbf{r}). \quad (21)$$

The auxiliary potentials  $W_i$  are obtained using the finite element method and the factorized Green's function and satisfy the linear systems

$$\mathbf{L}\mathbf{w}_i = 4\pi\mathbf{U}\mathbf{D}^{(i)}\mathbf{v}, \quad i = 1, \dots, \frac{N}{2} \quad (22)$$

with the diagonal matrices  $\mathbf{D}^{(i)}$  defined by

$$d_{jj}^{(i)} = v_j^{(i)}, \quad (23)$$

and where  $\mathbf{w}_i$  are the finite element vectors, whose components are the values of  $W_i$  at the interpolation grid points. Thus the Hartree potential requires one solution of the Poisson equation, while the exchange potential requires  $N/2$  solutions of the Poisson equation for every application to a wave function.

In order to uniquely specify these potentials boundary conditions are needed. For large enough  $r$  the Hartree potential must approach  $N/r$ , the Coulomb potential due to all electrons. The boundary conditions for the  $W_i$  are taken as vanishing at the outer surface of the domain. However the combined effect of both the Hartree and exchange potentials must for large values of  $r$  approach the Coulomb potential due to  $N - 1$  electrons. To enforce this long range behavior the boundary condition for the Hartree potential at the surface of the domain is instead chosen as  $(N - 1)/r$ . This boundary condition is applied via splitting the potential into the solution of the Poisson equation with zero boundary conditions and the regular solution of the Laplace equation with the above boundary condition, which is obtained using an expansion in terms of real-valued solid harmonics [11].

The finite element matrix  $\mathbf{V}_H$  corresponding to the Hartree potential is sparse and its calculation proceeds by evaluating  $V_H$  using the same  $F_j$  as used for the finite element calculations. However the exchange potential requires some approximation given its computational complexity. The expression for the matrix element of  $V_X$  between the finite element basis functions  $F_j$  and  $F_k$  reads

$$\int F_j V_X F_k d^3r = - \sum_{i=1}^{N/2} \int F_j \psi_i P(4\pi\psi_i F_k) d^3r, \quad (24)$$

where  $P$  is the operator that solves the Poisson equation with zero boundary conditions at the domain surface.

Replacing the wave functions  $\psi_i$  appearing in Eq. (24) by their finite element expansions and using Eq. (22), the effect of  $\mathbf{V}_X$  on a wave function vector  $\mathbf{v}$  in the finite element space becomes

$$(\mathbf{V}_X\mathbf{v})_j = - \sum_{k=1}^N \sum_{l=1}^N \sum_{i=1}^{N/2} \int F_j v_l^{(i)} F_l F_k 4\pi [\mathbf{L}^{-1}\mathbf{U}\mathbf{D}^{(i)}\mathbf{v}]_k d^3r. \quad (25)$$

Under the assumption that the wave functions  $\psi_k$  can be considered as slowly varying over distances of the order of the local grid spacing,  $\mathbf{V}_X$  is finally approximated by

$$\mathbf{V}_X = -4\pi \sum_{i=1}^{N/2} \mathbf{D}^{(i)} \mathbf{U} \mathbf{L}^{-1} \mathbf{U} \mathbf{D}^{(i)}. \quad (26)$$

This definition results in a symmetric operator as required.

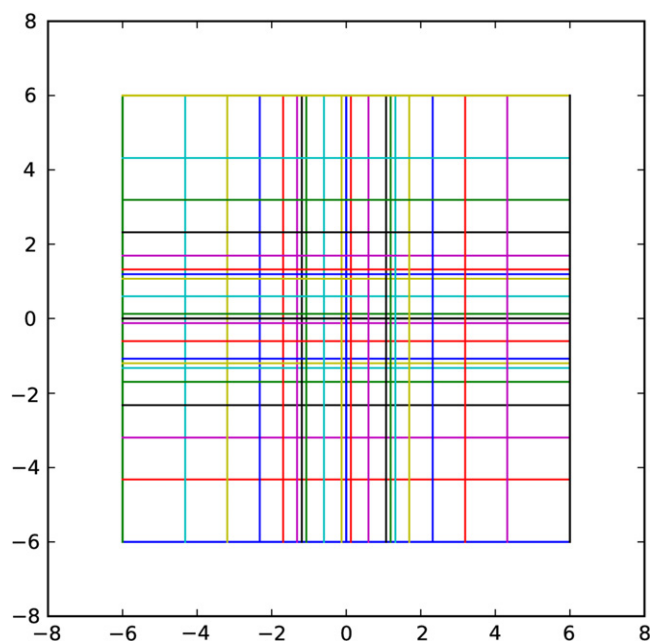


**Fig. 1.** Projection of the finite element grid for methane and  $h = 0.125$  onto the  $x$ - $y$ -plane. The outer portion of the grid for  $|x|$ ,  $|y|$  and  $|z| \geq 6$  has been removed for clarity.

### 3. Computational details

For the Hartree–Fock calculations tensor grids of order  $p = 3$  and  $p = 4$  were used. The nodes were compressed quadratically in the vicinity of the nuclei. The domain was chosen as  $[-x_{\max}, x_{\max}]^3$  with a large enough  $x_{\max}$ , determined by increasing this cutoff, until the energies do not change appreciably. The grids were identified by  $x_{\max}$  and the grid size  $h$  at the nuclei. For production runs the grid was divided into an outer region between  $|x|$ ,  $|y|$ ,  $|z| = \frac{1}{4}x_{\max}$  and  $x_{\max}$  covered with only one element in each direction and dimension and the inner region equivalent to the grid as above but with  $x_{\max}$  divided by four. In Fig. 1 a projection of the resulting grid for methane and  $h = 0.125$  on the  $x$ - $y$ -plane is shown.

The local finite element matrices were evaluated numerically using Gauss–Legendre integration. For the local kinetic energy and overlap matrices, the integration order was 12 in each coordinate for all elements. For the finite element matrices of the various potentials Gauss integration of order 12 was used in all elements that do not include a nucleus. For all elements that include a nucleus the integration was done in the coordinates  $\sqrt{|x|}$ ,  $\sqrt{|y|}$  and  $\sqrt{|z|}$ , where  $(x, y, z)$  is the distance vector from the nucleus and an integration of order 24 in each transformed coordinate was used. This was done to ensure convergence for the case of the nuclear Coulomb potential.

The code was written in Python [12], making use of the numpy [13] extensions for linear algebra and the pyparse extension [14] for handling sparse matrices and providing the Jacobi–Davidson eigenvalue solver.

As usual approximations of the wave functions and the Hartree–Fock energies were obtained using a self consistent field iteration and starting either from the bare nuclei and filling the molecule with two electrons at a time for non-degenerate orbitals, while in the case of degeneracies two electrons are added for each degenerate orbital, or using the wave functions of a previous calculation as input.

## 4. Results

### 4.1. Results for the atoms helium and beryllium

In order to test the method for the case of atoms, where highly accurate Hartree–Fock energies are available from calculations in a radial basis set, the atoms helium and beryllium were considered. For those atoms Hartree–Fock energies were calculated for a set of  $h$ -values chosen such that the nodes  $x_i$  between  $x = 0$  to  $x = \frac{1}{4}x_{\max}$  are of the form  $x_i = hi^2$ ,  $i = 0 \dots n$  with  $h = x_{\max}/(4n^2)$ . For helium the values were  $n = 2, 3, \dots, 8$  while for beryllium they were  $n = 3, 4, \dots, 8$ . This special choice of grids was required to enable fitting and extrapolation of the Hartree–Fock energy of as a function of  $h$ , since extrapolation requires a sufficiently regular sequence of grids. Choosing  $h$  values that do not satisfy the above conditions violates this condition.

In Figs. 2 and 3 least square fits of  $a + bh^c$  for the resulting Hartree–Fock energies for helium and beryllium are shown together with the resulting values for  $a$ ,  $b$  and  $c$ .

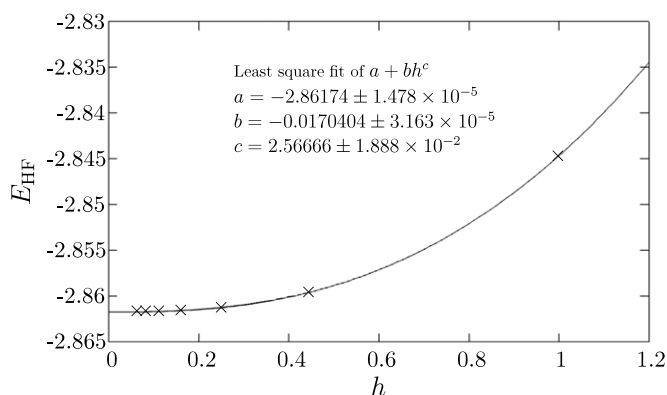


**Fig. 2.** Least square fit of  $a + bh^c$  of Hartree–Fock energy  $E_{\text{HF}}$  for helium. The crosses are the calculated values on the grid of  $h$ -values explained in the text.

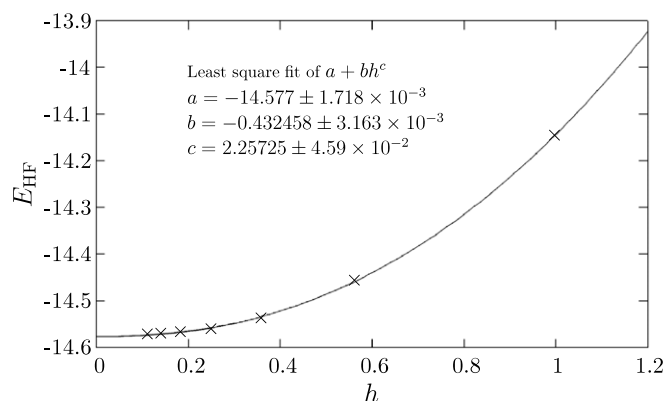


**Fig. 3.** Least square fit of  $a + bh^c$  of Hartree–Fock energy  $E_{\text{HF}}$  for beryllium. The crosses are the calculated values on the grid of  $h$ -values explained in the text.

**Table 1**  
Extrapolated HF energies for He and Be and literature values.

Atom	$E_{\text{HF}}^{\text{ext}}$	$E_{\text{HF}}^{\text{lit}}$
He	−2.86174	−2.861680 [16]
Be	−14.577	−14.573023 [17]

The least square fits are rather good and thus provide another example of extrapolation for finite element energies [15] and references therein, albeit here for non-integer exponents. The exponent  $c$  for beryllium is somewhat smaller than the one for helium.

In Table 1 the extrapolated energy values for  $h = 0$ , i.e.  $n \rightarrow \infty$ , which are given by the values of the constant term  $a$  are compared with literature values. The extrapolated values are slightly lower, than those from the literature, which is most probably due to some remaining errors in the numerical evaluation of integrals used to obtain the finite element matrices.

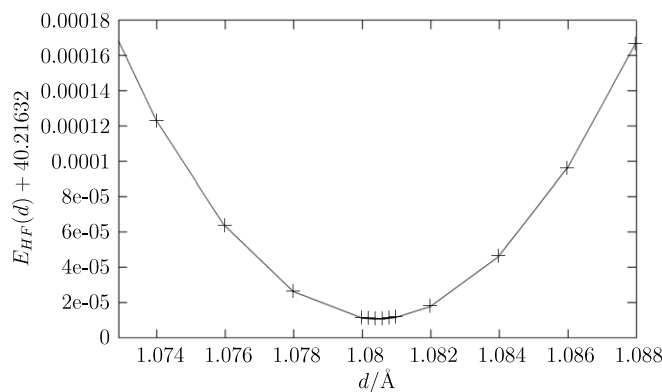
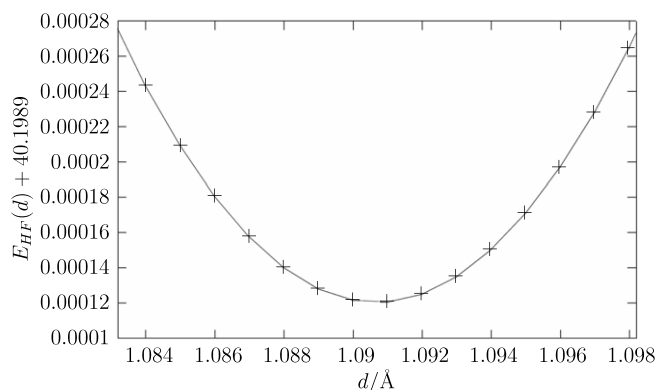
#### 4.2. Results for the molecules $\text{CH}_4$ , $\text{H}_2\text{O}$ and $\text{NH}_3$

In Table 2 finite element results for the Hartree–Fock ground state energies of the three molecules methane, water and ammonia are shown. They are presented together with results from calculations using Gaussian basis functions employing the open source computational chemistry package NWChem [18], experimental values and the discretization parameters of the finite element calculations. For the finite element calculations the self consistent iteration was stopped when  $|\Delta E_{\text{HF}}| < \epsilon$  with  $\epsilon = 10^{-6}$  for methane and  $\epsilon = 10^{-5}$  for water and ammonia. For methane the finite element Hartree–Fock energy was optimized with respect to the C–H-distance  $d$  and the minimum of this energy was found at  $d = 1.0804 \text{ \AA}$ , as shown in Fig. 4. The methane calculation using NWChem was also done over a range of values of  $d$  to find the optimal distance at  $d = 1.0907 \text{ \AA}$ , as shown in Fig. 5. At the experimental equilibrium distance of  $d = 1.0859 \text{ \AA}$  [19] the HF energies were obtained as −40.2162 and −40.1987 using the finite element code and NWChem respectively.

**Table 2**

Hartree–Fock ground state energies resulting from finite element and NWCHEM calculations, experimental ground state energies, discretization parameters and matrix order of the finite element calculations.

Molecule	$E_{\text{gs}}^{\text{FEM}}$	$E_{\text{gs}}^{\text{NWCHEM}}$	$E_{\text{gs}}^{\text{exp}}$	$x_{\text{max}}$	$h$	$\mathcal{N}$
CH <sub>4</sub>	−40.2163	−40.1988	−40.525	24	0.07	1 685 159
H <sub>2</sub> O	−76.0577	−76.0271	−76.483	24	0.0625	1 182 243
NH <sub>3</sub>	−56.2217	−56.1953	−56.588	24	0.06	1 854 567

**Fig. 4.** CH<sub>4</sub> Hartree–Fock energy as function of C–H distance  $d$  calculated using finite elements.**Fig. 5.** CH<sub>4</sub> Hartree–Fock energy as function of C–H distance  $d$  calculated using NWCHEM.

For both water and ammonia both the NWCHEM and finite element calculations used the experimental geometry. All NWCHEM calculations used the cc-pvdz basis set. The relative differences between the finite element and NWCHEM Hartree–Fock energies are smaller than 0.1%. The finite element calculations required CPU times of the order of 24 h while the NWCHEM calculations typically took less than a second.

Another parameter describing the methane molecule is the force constant  $F$  in the quadratic expansion  $E(d) = E_0 + \frac{F}{2}(d - d_0)^2$  around the equilibrium distance  $d_0$ . Least square fits for this expansion were done for both calculations with the results  $F_{\text{FEM}} = (5.468 \pm 0.01)$  Hartree/Å<sup>2</sup> and  $F_{\text{NWCHEM}} = (5.482 \pm 0.016)$  Hartree/Å<sup>2</sup>. They agree with each other to better than 1%, which again underscores the agreement between the two methods. To obtain the force constant  $F_{11}$  which is normally given in aJ/Å<sup>2</sup> and refers to one C–H bond only we use 1 Hartree = 4.359 aJ arriving at  $F_{11}^{\text{FEM}} = (5.959 \pm 0.011)$  aJ/Å<sup>2</sup> and  $F_{11}^{\text{NWCHEM}} = (5.974 \pm 0.017)$  aJ/Å<sup>2</sup> to be compared with the literature value  $F_{11} = 5.489$  aJ/Å<sup>2</sup> [19].

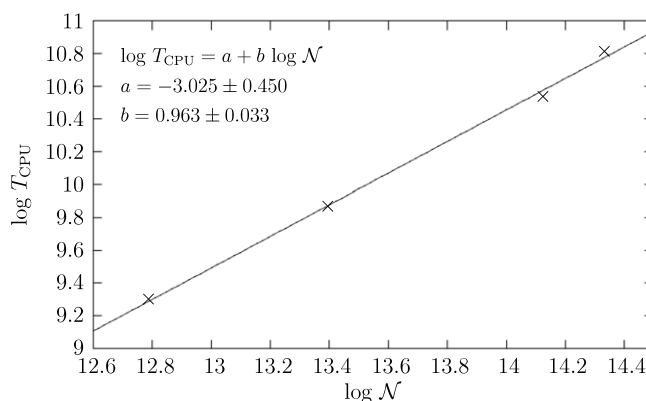
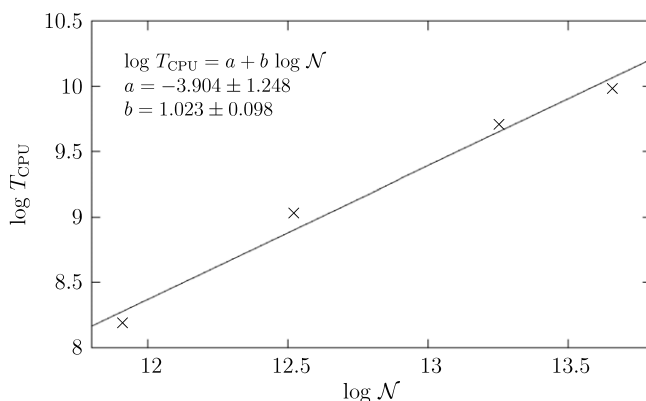
The calculations reported above all used  $p = 4$  and did not make use of extrapolation techniques for the sequence of energy values obtained in the self consistent iteration process. Thus these calculations used more CPU time than would have been required if using extrapolation. Therefore further calculations were done for both  $p = 3$  and  $p = 4$  as well as a number of  $h$ -values for CH<sub>4</sub> at the experimental C–H distance of  $d = 1.0859$  Å [19] and using the following extrapolation formula:

$$E_i^{\text{ext}} = E_i + \Delta E_i \frac{\alpha_i}{1 - \alpha_i}, \quad \alpha_i = \frac{\Delta E_i}{\Delta E_{i-1}}, \quad \Delta E_i = E_i - E_{i-1}, \quad i \geq 3. \quad (27)$$

**Table 3**

Extrapolated Hartree–Fock energies for the experimental geometry of methane for the indicated values of  $h$  and  $p$ . The last column indicates the CPU time required for the calculations.

$p$	$h$	$E_{\text{HF}}^{\text{ext}}$	$T_{\text{CPU}}/\text{s}$
3	0.06	−40.2044	21 634
3	0.09	−40.2014	16 447
3	0.125	−40.0383	8 312
3	0.25	−39.9326	3 583
3	0.5	−38.1067	1 996
4	0.07	−40.2162	49 850
4	0.09	−40.2141	37 688
4	0.125	−40.2003	19 264
4	0.25	−40.1417	10 980
4	0.5	−39.4837	6 020

**Fig. 6.** Least square fit of  $\log T_{\text{CPU}} = a + b \log \mathcal{N}$  for  $p = 4$ .**Fig. 7.** Least square fit of  $\log T_{\text{CPU}} = a + b \log \mathcal{N}$  for  $p = 3$ .

The self consistent iteration was terminated, when the difference between successive extrapolated energy values was less than  $5 \times 10^{-5}$ , indicating convergence of the extrapolated energy to 4 decimals after the point.

In the following tables  $E_{\text{HF}}^{\text{ext}}$  obtained for the indicated values of  $p$  and  $h$  is given together with the CPU time required. The calculations for  $h = 0.5$  and  $p = 4$  started with the bare nuclei, while those for smaller  $h$ -values and for  $h = 0.5$  and  $p = 3$  used the wave function obtained for  $h = 0.5$  and  $p = 4$  as input. From the Hartree–Fock energies given in this table, it is evident, that reasonably accurate values can be obtained using, for example,  $p = 3$  and  $h = 0.09$ .

In Figs. 6 and 7 the CPU times shown in Table 3 are plotted against the matrix size  $\mathcal{N}$  in a double logarithmic plot together with a least square fit of  $\log T_{\text{CPU}} = a + b \log \mathcal{N}$ . In both cases the exponent  $b$  is of the order of 1.0, demonstrating that the time taken for eigenvalue calculations scales approximately linearly with  $\mathcal{N}$ . For both fits the time taken for the smallest value of  $\mathcal{N}$  was disregarded, as the calculation for  $p = 4$  and  $h = 0.5$  started with the bare nucleus to provide a starting wave function.

Since the chosen molecular grids are not sufficiently regular, extrapolation to  $h = 0$  is not feasible.



## 5. Conclusions

The computational procedure that was developed to solve the closed shell Hartree–Fock equations has been explained in some detail.

Results of finite element closed shell Hartree–Fock calculations for the atoms helium and beryllium, and the molecules methane, water and ammonia have been presented and compared with very accurate literature results for the atoms and results obtained using the open source computational chemistry package NWChem for the molecules. The resulting energies show excellent agreement. However the computational effort for the finite element calculations is much greater than the effort when using a Gaussian basis set package such as NWChem, especially if high accuracy is required. Thus this method is not suitable as a replacement for Gaussian basis set calculation but rather in order to obtain wave functions with better asymptotic properties using the result of NWChem calculation as input.

For the atoms helium and beryllium it was established, that the Hartree–Fock energies can be fitted to  $E(h) = a + bh^c$  with good accuracy. It has also been shown, that the CPU time scales approximately linearly with the matrix dimension  $\mathcal{N}$ . To accelerate the finite element calculations it is planned to parallelize the computation of the matrix elements using OpenMP and/or MPI.

## Acknowledgments

Financial support by the National Research Foundation (NRF) of South Africa and by the University of South Africa (UNISA) is acknowledged.

## References

- [1] L. Ram-Mohan, Finite Element and Boundary Element Applications in Quantum Mechanics, in: Oxford Texts in Applied and Engineering Mathematics, Oxford University Press, Oxford, UK, 2002.
- [2] D. Heinemann, D. Kolb, B. Fricke,  $H_2$  solved by the finite element method, Chem. Phys. Lett. 137 (1987) 181–183.
- [3] D. Heinemann, B. Fricke, D. Kolb, Solution of the Hartree–Fock–Slater equations for diatomic molecules by the finite-element method, Phys. Rev. A 38 (1988) 4994–5001.
- [4] R. Alizadegan, K.J. Hsia, T.J. Martinez, A divide and conquer real space finite-element Hartree–Fock method, J. Chem. Phys. 132 (2010) 034101.
- [5] C. Froese-Fischer, The Hartree–Fock Method for Atoms: A Numerical Approach, Wiley, New York, 1977.
- [6] G.L.G. Sleijpen, H.A. van der Horst, A Jacobi–Davidson iteration method for linear eigenvalue problems, SIAM J. Matrix Anal. Appl. 17 (1996) 401–425.
- [7] P. Arbenz, R. Geus, A comparison of solvers for large eigenvalue problems originating from Maxwell's equations, Numer. Linear Algebra Appl. 6 (1999) 3–16.
- [8] N.W. Schellingerhout, Factorizability in the numerical few-body problem, Ph.D. Thesis, University of Groningen, The Netherlands, 1995.
- [9] R.J.F. Berger, D. Sundholm, A non-iterative numerical solver of Poisson and Helmholtz equations using high-order finite-element functions, Adv. Quantum Chem. 50 (2005) 235–246.
- [10] M. Braun, Different approaches to the numerical solution of the 3D Poisson equation implemented in Python, Computing 95 (2013) S49–S60.
- [11] L. Surhone, M. Tennoe, S. Henssonow, Solid Harmonics, VDM Publishing, 2010.
- [12] 2013. <http://www.python.org>.
- [13] 2013. <http://numpy.scipy.org>.
- [14] 2013. <http://pysparse.sourceforge.net>.
- [15] L. Qun, X. Hehu, Extrapolation of the finite element method on general meshes, Int. J. Numer. Anal. Model. 10 (2013) 139–153.
- [16] C.C.J. Roothaan, L.M. Sachs, A.W. Weiss, Analytical self-consistent field functions for the atomic configurations  $1s^2$ ,  $1s^2 2s$ , and  $1s^2 2s^2$ , Rev. Modern Phys. 32 (1960) 186–194.
- [17] E. Lindroth, H. Persson, S. Salomonson, A.-M. Mårtensson-Pendrill, Corrections to the beryllium ground-state energy, Phys. Rev. A 45 (1992) 1493–1496.
- [18] M. Valiev, E. Bylaska, N. Govind, K. Kowalski, T. Straatsma, H.V. Dam, D. Wang, J. Nieplocha, E. Apra, T. Windus, W. de Jong, Nwchem: a comprehensive and scalable open-source solution for large scale molecular simulations, Comput. Phys. Comm. 181 (2010) 1477–1489.
- [19] J.F. Stanton, A refined estimate of the bond length of methane, Mol. Phys. 97 (1999) 841–845.